Inorganic Chemistry

Article

pubs.acs.org/IC

Erbium Hydroxide Ethanedisulfonate: A Cationic Layered Material with Organic Anion Exchange Capability

Kevin M. Sergo, Cari S. Han, Marc R. Bresler, Susan C. Citrak, Yashar Abdollahian, Honghan Fei, and Scott R. J. Oliver*

Department of Chemistry and Biochemistry, University of California, Santa Cruz, 1156 High Street, Santa Cruz, California 95064, United States

Supporting Information

ABSTRACT: We describe a cationic erbium-based material $[Er_{12}(OH)_{29}(H_2O)_5][O_3SCH_2CH_2SO_3]_{3.5}\cdot 5H_2O$. As synthesized, the material is water stable and capable of complete organic anion exchange for a variety of α,ω-alkanedicarboxylates. We chose these anions as initial examples of exchange and as an analog for pharmaceutical waste, some of which have a carboxylate functionality at neutral pH range. Free-floating and partially anchored organosulfonate anions reside between the cationic corrugated layers and allow for exchange. The structure also displays a reversible hydration event above 100 °C. Both the as-synthesized and the exchanged materials are characterized by a variety of analytical techniques.

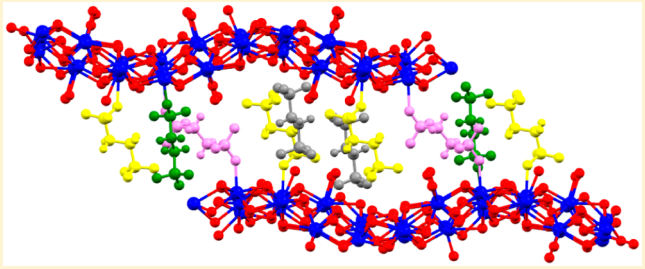

INTRODUCTION

Organic water-borne pollutants are generated through both industrial and personal use. The U.S. Environmental Protection Agency (EPA) classifies many of these wastes as Pharmaceutical and Personal Care Products (PPCPs).[1] This includes prescription, over-the-counter, and veterinary drugs, as well as vitamin supplements, cosmetics, and medical diagnostic agents. Pharma wastes consist of the active pharmaceutical ingredients (APIs), metabolites or conjugates of the API, and excipients that act as carriers and fillers. The fate of these compounds is often wastewater with one of the main routes being simple excretion. Hospitals are one of the largest sources due to the high density of patients and throughput of drugs. Accidental releases of organic compounds, such as the Elk River chemical spill, are also of great concern due to the volume and concentration associated with their release.[2] Wastes that are stable in the environment may bioaccumulate in flora or fauna.[3−5] Biomagnification of pollutants through the food chain is of concern due to the effect it can have on the ecosystem. Wastes that are natively anionic at neutral pH are particularly troublesome due to a lack of adequate cationic traps.[7] Resins and organically functionalized zeolites are the most used anion exchange media but suffer from lack of chemical and thermal stability due to the organic component and are not reusable for most anions.[8,9] Development of materials for use in remediation efforts for both spills and regular low-level releases through excretion is important for protecting our environment.

Layered double hydroxides (LDHs) are a heavily studied class of compounds consisting of cationic inorganic layers charge balanced by anions in the interlamellar space. They follow the general formula $[M^{2+}_{1-x}M^{3+}_{x}(OH)_2][A^{n-}_{x/n}\cdot mH_2O]$, where M^{2+} and M^{3+} are a range of metals (typically Mg^{2+} and Al^{3+}), x is the ratio of $M^{3+}/(M^{2+} + M^{3+})$, and n is the charge of the interlamellar anions.[10,11] LDHs are capable of anion uptake which is enhanced by precalcination. Most LDHs suffer from the fact that they partially adsorb the carbonate anion over the anionic pollutant of interest as well as the need for an energy-intensive precalcination and postcentrifugation.

Lanthanides have been studied as dopants for LDHs but also as the metal building block for related cationic materials. Haschke discovered a series of lanthanide hydroxynitrates in the 1970s[12] that have been studied more extensively in recent years for anion exchange.[13] These studies have led to new lanthanide hydroxynitrates, hydroxyhalides, and hydroxides as reported by Fogg and co-workers[14−16] as well as Gutierrez-Puebla, Monge, and co-workers.[17] The materials have cationic lanthanide hydroxide layers balanced by inorganic or organic anions and display rich intercalation chemistry with organic dicarboxylates and disulfonates. Recently, Feng and co-workers reported an indium-based metal−organic framework that exchanges its nitrate for a variety of organic dyes.[18] Another emerging class of cationic materials developed by Albrecht-Schmitt and co-workers is actinide borates capable of pertechnetate trapping.[19] Custelcean has also shown anion trapping by a highly adaptable method of selective crystallization.[20] Previously, our group published a series of transition-metal-based cationic materials[7,21−25] that are thermally and chemically stable in water and unlike LDHs are not subject to carbonate interference, allowing the study of actual wastewater. For example, 50-fold excess carbonate prevented any chromate uptake by calcined hydrotalcite LDH, with the chromate

Received: January 9, 2015
Published: April 7, 2015

DOI: 10.1021/acs.inorgchem.5b00073
Inorg. Chem. 2015, 54, 3883−3888

capacity dropping from 17 to 0 mg/g. The chromate uptake by our "$Zn_{0.5}Co_{0.5}$-SLUG-35" remained at 68.5 mg/g in the presence of carbonate, and no carbonate was observed in the FTIR of the solid.[24b]

Herein, we report our first rare-earth-based cationic material that is capable of complete organic anion exchange. A variety of α,ω-alkanedicarboxylates were exchanged as analogs for anionic pharmaceutical pollutants. The weak interaction between the interlamellar organic anion and the cationic erbium hydroxide layers allows for the exchange. The material also displays a reversible hydration event up to 200 °C that may further enhance the anion exchange capabilities.

EXPERIMENTAL SECTION

Reagents. Erbium(III) chloride hydrate ($ErCl_3{\cdot}xH_2O$, Alfa Aesar, 99.9%), 1,2 ethanedisulfonate disodium salt ($NaO_3SCH_2CH_2SO_3Na$, Acros Organics, 99%), and triethylamine [$N(CH_2CH_3)_3$, Aldrich, 99%] were used as received for the synthesis. Malonic acid ($HO_2CCH_2CO_2H$), succinic acid [$HO_2C(CH_2)_2CO_2H$], glutaric acid [$HO_2C(CH_2)_3CO_2H$], adipic acid [$HO_2C(CH_2)_4CO_2H$], *p*-terephthalic acid [$HOOC(C_6H_4)COOH$], 2,6-naphthalene disulfonic acid [$NaO_3S(C_{10}H_6)SO_3Na$, Sigma-Aldrich, 99%], and 2,6-naphthalene dicarboxylic acid [$HO_2C(C_{10}H_6)CO_2H$] were used as received for the anion exchange reactions (all TCI America, 99%).

Synthesis. Pink crystals of $[Er_{12}(OH)_{29}(H_2O)_5][O_3SCH_2CH_2SO_3]_{3.5}{\cdot}5H_2O$ (which we denote as SLUG-27: University of California, Santa Cruz, structure no. 27) were synthesized under hydrothermal conditions. A mixture of $ErCl_3{\cdot}xH_2O$ (1.22g), $NaO_3SCH_2CH_2SO_3Na$ (0.22g), triethylamine (0.42 g), and deionized water (10 mL) was weighed into a 15 mL capacity autoclave (2/3 capacity). The autoclave was heated statically at either 175 °C for 5 days or 200 °C for 2 days under autogenous pressure. After cooling to room temperature, a pink solid consisting of larger needle-like crystals dispersed among smaller more fibrous crystals was obtained via vacuum filtration. The product was rinsed with DI H_2O and acetone.

Anion Exchange. A 100 mg amount of of SLUG-27 solid was placed in 10 mL of deionized water containing a 3-fold molar excess (with respect to SLUG-27) of malonic, succinic, glutaric, adipic, *p*-terephthalic, or 2,6-naphthalene dicarboxylic acid. The reaction mixture was left covered for 24 h under mild stirring. The solid products were collected via vacuum filtration and rinsed with DI H_2O/acetone.

Instrumental Details. Single-crystal data were collected on a Bruker APEX II CCD area detector X-ray diffractometer using graphite-monochromated Mo Kα radiation (λ = 0.71073 Å). The structures were solved by direct methods and expanded routinely. The models were refined by full-matrix least-squares analysis of F^2 against all reflections. All non-hydrogen atoms were refined with anisotropic thermal displacement parameters. Thermal parameters for the hydrogen atoms were tied to the isotropic thermal parameter of the atom. Powder X-ray diffraction (PXRD) spectra were obtained on a Rigaku Miniflex II Plus with Cu Kα radiation (λ = 1.5418 Å) from 2° to 40° (2θ) at a rate of 2° per minute and a 0.04° step size. In-situ variable-temperature PXRD (VT-PXRD) was performed on a Rigaku SmartLab X-ray Diffractometer with Cu Kα radiation (λ = 1.5405 Å) from 2° to 40° (2θ) at a rate of 2° per minute and a 0.02° step size. The samples were heated at a rate of 10 °C/min and held at the set temperature for 5 min before scanning. Thermogravimetric analysis (TGA) was performed on a TA Thermoanalyzer 2050. Samples were heated in an aluminum pan with a Pt wire at a ramp rate of 10 °C/min. For cyclic TGA, the same ramp rate was used for cooling but the oven took much longer to cool back to 25 °C. Fourier transform infrared (FTIR) spectroscopy of the materials was collected on a PerkinElmer Spectrum One spectrophotometer using KBr pellets.

RESULTS AND DISCUSSION

Synthesis. Pink crystals of SLUG-27 were obtained hydrothermally as a pure phase at both 175 and 200 °C. The product consisted of larger needlelike crystals dispersed among smaller more fibrous crystals in an approximately equal ratio as observed by optical microscopy. The material forms as mat-like aggregates near the surface of the reaction mixture in the autoclave. No nitrogenous species were present in the obtained structure, further indicating that the triethylamine served solely as a pH modifier. If no triethylamine was added, only starting materials were obtained.

Structure Characterization. Single-crystal X-ray diffraction reveals corrugated cationic erbium hydroxide layers balanced by anionic ethanedisulfonate (EDS, Figure 1) in a

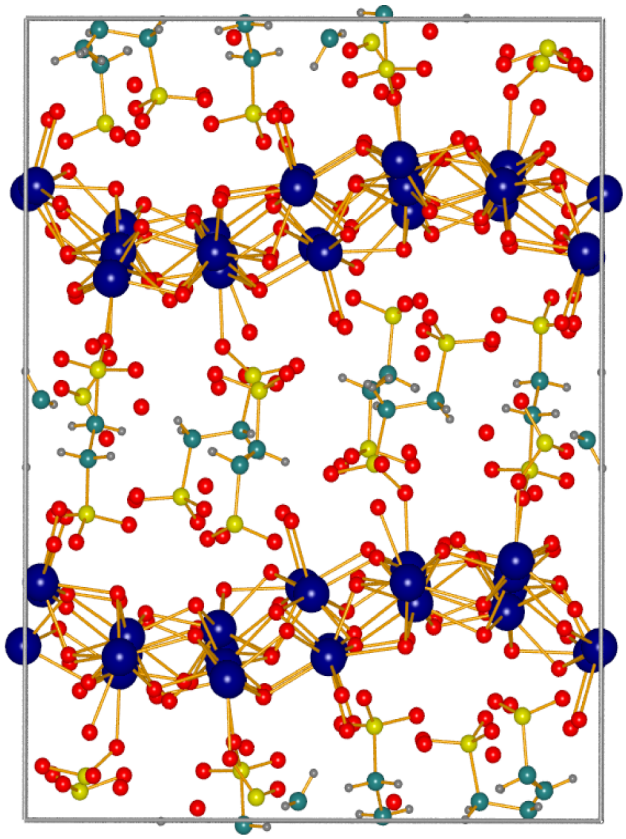

Figure 1. Crystallographic *a* projection of SLUG-27, showing the corrugated layers end on and the interlamellar EDS anions (Er, blue; O, red; S, yellow; C, teal). Layer hydrogens omitted for clarity.

$P2_1/c$ space group (Table 1). Experimental PXRD fully matched the theoretical PXRD calculated from the single-crystal data (Figure S1, Supporting Information). The erbium hydroxide layers are very low in symmetry, with 12 crystallographically independent erbium centers (Figure 2). Three erbium centers are distorted pentagonal bipyramidal, while the remaining nine are distorted square antiprismatic (Figure S2, Supporting Information). The EDS molecules balance the positive charge of the layer and covalently interact in four ways (Figure S3, Supporting Information): singly bound (two crystallographically independent instances), doubly bound (one instance), and floating (unbound, one instance). These multiple modes of connectivity for the sulfonate headgroup have been observed in our cationic MOFs templated by EDS[22−25] as well as organosulfonate-containing MOFs

DOI: 10.1021/acs.inorgchem.5b00073
Inorg. Chem. 2015, 54, 3883−3888

Table 1. Crystal Data and Structure Refinement for SLUG-27

empirical formula	$Er_{12}O_{55}S_7C_7H_{14}$
fw	3209.79
T	296(2) K
wavelength	0.71073 Å
cryst syst	monoclinic
space group	$P2_1/c$
unit cell dimens	a = 14.0296(4) Å
	b = 23.8117(7) Å
	c = 18.3099(5) Å
	α = 90°
	β = 100.04°
	γ = 90°
vol.	6023.0(3) Å^3
Z	1
density (calcd)	3.646 g·cm^{-3}
abs coeff (μ)	16.882 mm^{-1}
F(000)	5886
cryst size	0.125 × 0.055 × 0.045 mm^3
ω range for data collection	1.90–24.71°
index ranges	$-16 \le h \le 16$, $-28 \le k \le 28$, $-21 \le l \le 21$
no. of reflns collected	10 277
no. of independent reflns	8161 [R_{int} = 0.0652]
completeness to θ = 24.71°	99.9%
abs corr	empirical
max and min transmission	0.7452 and 0.4476
refinement method	full-matrix least squares on F^2
data/restraints/params	10 277/18/776
goodness-of-fit on F^2	1.030
final R indices [$I > 2\sigma(I)$]	R_1 = 0.0319, wR_2 = 0.0655
R indices (all data)	R_1 = 0.0467, wR_2 = 0.0720
largest diff. peak and hole	1.424 and −1.305 e$^-$·Å^{-3}

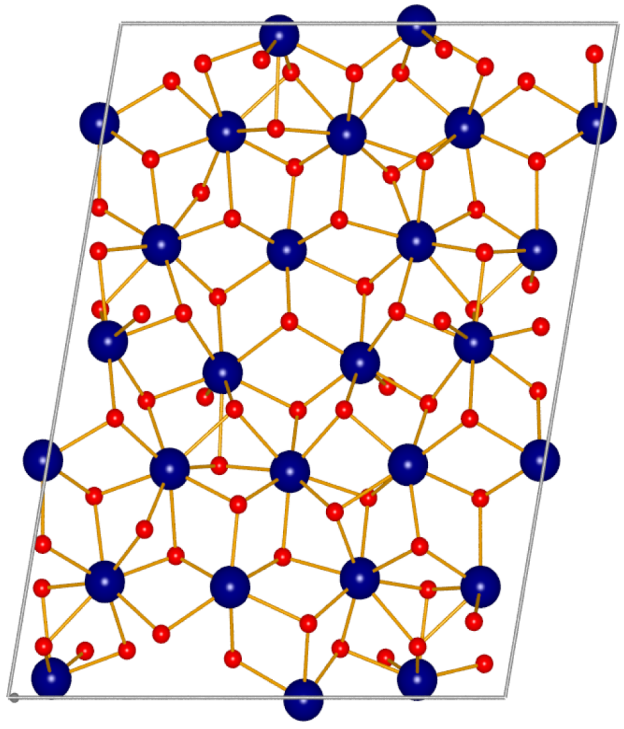

Figure 2. Crystallographic b projection of one inorganic $[Er_{12}(OH)_{29}(H_2O)_5]$ layer (Er, blue; O, red). Hydrogen atoms omitted for clarity.

reported by others such as those of Shimizu and co-workers.[26] For the two singly bound EDS anions, one oxygen covalently bonds to an erbium of the layer [2.29(1) and 2.31(1) Å]. The EDS oxygens are involved in a hydrogen-bonding network with the protonated layer and interlayer water (Figures 1 and S3, Supporting Information). The two doubly bound EDS molecules are crystallographically symmetrical about the carbon−carbon bond on the edge of the unit cell; hence, there are 3.5 EDS molecules in the formula. Of the 59 oxygen atoms in the asymmetric unit, 21 are from the 3.5 EDS molecules and 5 are free water molecules in the interlayer space. The remaining 34 oxygen atoms make up the erbium hydroxide lattice, with 5 terminal doubly protonated oxygens, 28 triply bridging, and 1 doubly bridging.

Anion Exchange. The intercalation chemistry of this new material was investigated using α,ω-alkanedicarboxylates of varying chain length. A 3-fold molar excess aqueous solution of the dicarboxylate was used to study the exchange properties, and the resultant solids were analyzed via FTIR spectroscopy and PXRD (see Experimental Section). FTIR spectroscopy clearly shows the disappearance of the sulfonate peaks (1200, 1070 cm^{-1}) and appearance of carboxylate peaks (1570, 1400 cm^{-1}) in all exchanged materials (Figure 3). The presence of the broad band ranging from 3500 to 3000 cm^{-1} in all spectra is indicative of the hydroxyl groups present on the erbium layers.

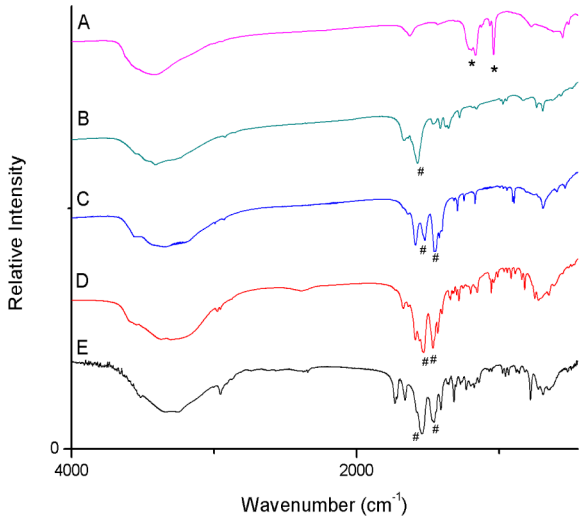

Figure 3. FTIR spectra of SLUG-27: (A) as synthesized; (B) exchanged with malonate [$^-O_2CCH_2CO_2^-$]; (C) exchanged with succinate [$^-O_2C(CH_2)_2CO_2^-$]; (D) exchanged with glutarate [$^-O_2C(CH_2)_3CO_2^-$]; (E) exchanged with adipate [$^-O_2C(CH_2)_4CO_2^-$]: (*) sulfonate peaks; (#) carboxylate peaks.

From the PXRD spectra of the exchanged materials (Figures 4 and S4, Supporting Information), the interlayer distances increased as expected with the chain length of the dicarboxylates (malonate < succinate < glutarate < adipate), with the exception of succinate (Table 2).[9,12] The principal peak of the as-synthesized material is at 7.60° 2θ, giving a layer-to-layer distance of 11.5 Å. On the basis of the relative carbon chain length and size of sulfonate versus carbonate end groups, it was expected that the adipate [$^-O_2C(CH_2)_4CO_2^-$] and glutarate [$^-O_2C(CH_2)_3CO_2^-$] would shift the principal (020) peak to lower 2θ values as the interlayer distance would increase, whereas succinate [$^-O_2C(CH_2)_2CO_2^-$] and malonate [$^-O_2CCH_2CO_2^-$] would have shorter interlayer distance.

DOI: 10.1021/acs.inorgchem.5b00073
Inorg. Chem. 2015, 54, 3883−3888

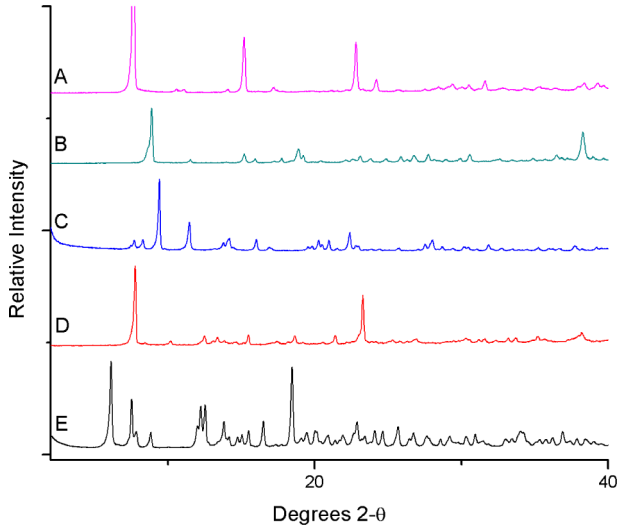

Figure 4. PXRD spectra of SLUG-27: (A) as synthesized; (B) exchanged with malonate [$^{-}O_2CCH_2CO_2^{-}$]; (C) exchanged with succinate [$^{-}O_2C(CH_2)_2CO_2^{-}$]; (D) exchanged with glutarate [$^{-}O_2C(CH_2)_3CO_2^{-}$]; (E) exchanged with adipate [$^{-}O_2C(CH_2)_4CO_2^{-}$].

Table 2. Data (2θ and d-spacing values) for SLUG-27 and the Exchanged Materials

anion	2θ (deg)	d spacing (Å)
as synthesized	7.6	11.6
malonate	8.9	9.9
succinate	9.4	9.4
glutarate	7.8	11.3
adipate	6.1	14.5

Instead, glutarate shifted the principal (020) peak very little, while succinate and malonate did shift to higher 2θ value, and succinate unexpectedly gave a higher value (Table 2). The smaller layer-to-layer distance for succinate is likely due to crystal packing, with succinate residing at a greater angle with respect to the layers. As expected, adipate shifted the principal peak to the lowest angle of the dicarboxylates (Table 2). The adipate phase contains a significant number of new PXRD peaks (Figure 4E), meaning the layer topology has likely changed, perhaps due to intralayer condensation of the terminal water molecules. Polycrystals are formed upon intercalation however, preventing single-crystal structure solution. Nevertheless, the appearance of carboxylate peaks in the IR spectra directly confirms that exchange has taken place. Attempts to reverse the exchange have been unsuccessful to date. 2,6-Naphthalenedisufonate, however, successfully intercalated into SLUG-27 at 50 °C, forming a new PXRD pattern (Figure S5, Supporting Information). 2,6-Naphthalenedicarboxlyate was insoluble even at 50 °C, so it did not intercalate.

Attempts to intercalate other aromatic dicarboxylates (e.g., *p*-terephthalate) were not successful, likely due to the limited aqueous solubility of these analytes at neutral pH. In this case, the product was a mixture of the unexchanged solid and the aromatic dicarboxylate in solid form. Indeed, FTIR spectra of the mixed solid shows the presence of both carboxylate and sulfonate groups, further confirming that exchange has not taken place. Others have reported the intercalation of *p*-terephthalate into cationic materials in basic aqueous solution.[27,28]

Thermal Properties. In-situ VT-PXRD (Figure 5) and TGA (Figure S6, Supporting Information) were used to further characterize the anion exchange capabilities. SLUG-27 is stable to ~300 °C as water is driven out of the interlamellar space. The visible peak broadening and loss of intensity indicates reduced crystallinity as the hydrogen-bonding network between the sulfonate groups and layers is likely lost. Indeed, the principal peak shifts to higher 2θ values, and the higher angle fine structure is largely lost (Figure 5). Above 300 °C, an amorphous material is observed with no sharp peaks. Above 700 °C, new peaks begin to form at 17−33° 2θ, which are indicative of erbium oxide (29.28° and 33.94° 2θ, ICDD #94-888). Slight thermal expansion occurs upon further heating, with the final room temperature scan shifting the peaks back to higher angle.

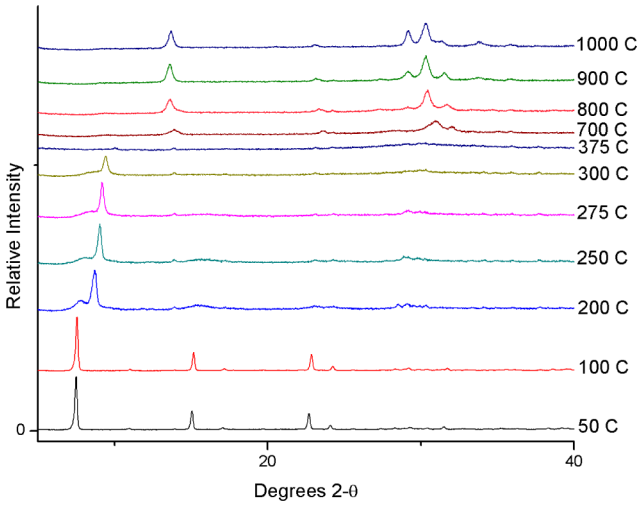

Figure 5. In-situ VT-PXRD of SLUG-27. Scans at 400, 425, 500, and 600 °C were identical to the primarily amorphous scan at 375 °C and are omitted for clarity.

VT-PXRD of the succinate-exchanged material (Figure 6) yielded similar behavior as the as-synthesized material. The

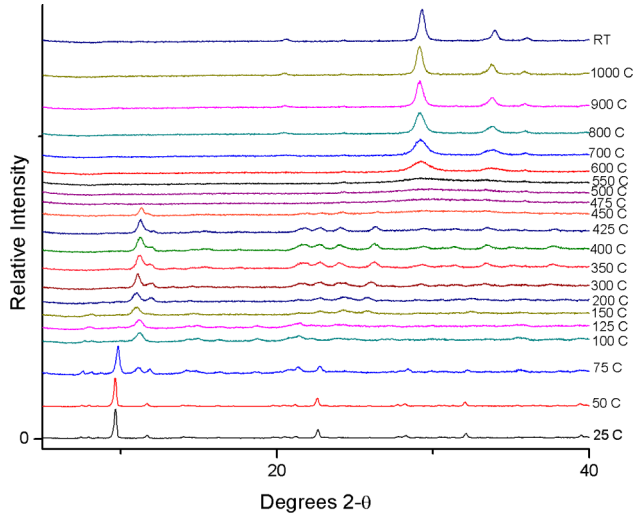

Figure 6. In-situ VT-PXRD of SLUG-27-succinate. RT is a room-temperature scan taken ~24 h after heating to 1000 °C. The peak visible at ~30° 2θ is indicative of erbium oxide (29.28° 2θ, ICDD #94-888).

DOI: 10.1021/acs.inorgchem.5b00073
Inorg. Chem. 2015, 54, 3883−3888

same gradual loss of crystallinity was observed up to ~450 °C before becoming completely amorphous, which corresponds to the significant mass loss in the TGA of the exchanged material (Figure S7, Supporting Information). At 600 °C, erbium oxide begins to form, with increased crystallinity as the temperature increased to 1000 °C. These observations are further confirmation of the complete and clean exchange of dicarboxylates for the EDS.

The gradual loss of crystallinity and shift of the principal peak to higher angle observed at lower temperature was further investigated by VT-PXRD, with a scan every 10 °C between 100 and 200 °C (Figure 7). The loss of water again led to peak

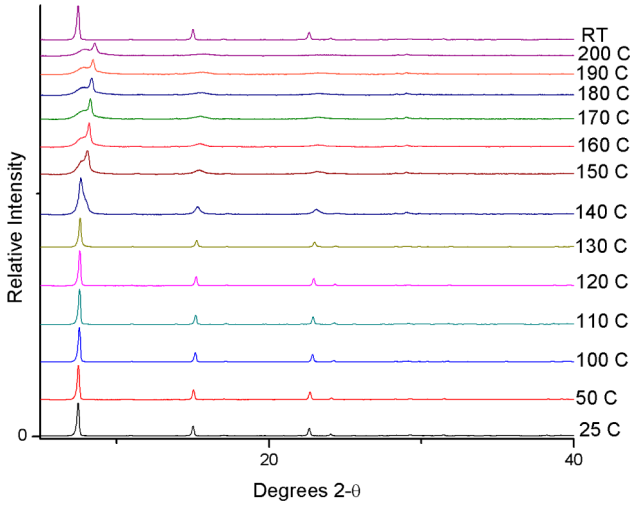

Figure 7. In-situ VT-PXRD of SLUG-27 from 25 to 200 °C. RT is a scan taken ~24 h after allowing the sample to cool back to room temperature.

broadening and a shift to higher angle, as expected. After resting for 24 h, the sample fully rehydrated and yielded the same spectrum as the starting pattern before heating (top pattern, Figure 7). This reversible dehydration/hydration event was studied further by TGA and showed a 3.4 wt % mass loss (Figure S8, Supporting Information). The five crystallographic waters in the interlayer region correspond to 2.2 wt %, with another five terminal waters on the layers. It is likely that all of the former along with physisorbed water are lost and the material is partially dehydrated. Indeed, VT-PXRD of SLUG-27 (Figure 5) shows that water loss continues up to ~275 °C. Two subsequent TGA runs on the rehydrated material showed a mass loss of 2.9 and 2.8 wt % over the same temperature region (Figure S8, Supporting Information). Lower percentages of mass loss are expected due to incomplete rehydration in the time between the trials. PXRD of the material after TGA to 200 °C indicated that at least 4 h are required under ambient conditions for complete rehydration and return to the original fully crystalline material. Some MOF materials have exhibited the ability to undergo dehydration/hydration and been used for drying various solvents.[29]

VT-PXRD and TGA analysis underscore the importance of the hydrogen-bonding network in the interlamellar space of SLUG-27. As water evolved, partial loss of crystallinity was observed. If this water was not contributing to the hydrogen-bonding stabilization, we would expect to see loss of mass in TGA but minimal changes to the PXRD spectra. Instead, as interlayer water is driven out, loss of mass (TGA) and concomitant reduction in crystallinity (VT-PXRD) were observed.

CONCLUSIONS

SLUG-27 is an erbium hydroxide cationic material that demonstrates complete organic anion exchange for α,ω-alkanedicarboxylates. We are currently studying the reversibility and intercalation of other organic and inorganic anions. Recapture of the native EDS anion after exchange has been successful and reused for further synthesis of material. As the usage of pharmaceutical products continues to expand, we must pay attention to the unintended consequences of these powerful bioactive compounds. Without the development of materials like SLUG-27 and other robust anion exchange materials we may not be able to ensure that the very compounds extending our lifespan and quality of life will have a detrimental effect on the future of our ecosystems that support us.

ASSOCIATED CONTENT

Supporting Information

Experimental and projected powder XRD patterns, ORTEP, TGA and crystallographic information This material is available free of charge via the Internet at http://pubs.acs.org. This material is available free of charge via the Internet at http://pubs.acs.org.

AUTHOR INFORMATION

Corresponding Author

*E-mail: soliver@ucsc.edu.

Notes

The authors declare no competing financial interest.

ACKNOWLEDGMENTS

The SCXRD and PXRD data in this work were recorded on instruments supported by the NSF Major Research Instrumentation (MRI) Program under Grant CHE-0521569 and DMR-1126845, respectively. We also thank Dr. Indranil Chakraborty for assistance with refinement of single crystal XRD data.

REFERENCES

(1) Daughton, C. G. EPA infographic: Pharmaceuticals and Personal Care Products, March 2006. http://www.epa.gov/ppcp/pdf/drawing.pdf.
(2) Cooper, W. J. *Environ. Sci. Technol.* **2014**, *48*, 3095−3095.
(3) Zuccato, E.; Calamari, D.; Natangelo, M.; Fanelli, R. *Lancet.* **2000**, *367*, 23−41.
(4) US Environmetnal Protection Agenge website, Pharmacueticals and Personal Care Products (PPCPs), Frequent Questions, Oct 2010. http://www.epa.gov/ppcp/faq.html.
(5) Crane, M.; Watts, C.; Boucard, T. *Sci. Total Environ.* **2006**, *367*, 23−41.
(6) Kümmerer, K. *Chemosphere* **2001**, *45*, 957−969.
(7) Oliver, S. R. J. *Chem. Soc. Rev.* **2009**, *38*, 1868−1881 and references therein.
(8) Haggerty, G. M.; Bowman, R. S. *Environ. Sci. Technol.* **1994**, *28*, 452−458.
(9) Humbert, H.; Gallard, H.; Suty, H.; Croué, J.-P. *Water Res.* **2005**, *39*, 1699−1708.
(10) Burrueco, M. I.; Mora, M.; Jiménez-Sanchidrián, C.; Ruiz, J. R. *J. Mol. Struct.* **2013**, *1034*, 38−42.
(11) Ulibarri, M. A.; Pavolvic, I.; Barriga, C.; Hermosin, M. C.; Cornejo, J. *Appl. Clay Sci.* **2001**, *18*, 17−27.

DOI: 10.1021/acs.inorgchem.5b00073
Inorg. Chem. 2015, 54, 3883−3888

(12) Haschke, J. M. *Inorg. Chem.* **1974**, *8*, 1812−1818.
(13) Geng, F.; Ma, R.; Sasaki, T. *Acc. Chem. Res.* **2010**, *9*, 1177−1185.
(14) McIntyre, L. J.; Jackson, L. K.; Fogg, A. M. *Chem. Mater.* **2008**, *20*, 335−340.
(15) Poudret, L.; Prior, T. J.; McIntyre, L. J.; Fogg, A. M. *Chem. Mater.* **2008**, *20*, 7447−7453.
(16) Goulding, H. V.; Hulse, S. E.; Clegg, W.; Harrington, R. W.; Playford, H. Y.; Walton, R. I.; Fogg, A. M. *J. Am. Chem. Soc.* **2010**, *132*, 13618−13620.
(17) Gandara, F.; Perles, J.; Snejko, N.; Igelsias, M.; Gomez-Lor, B.; Gutierrez-Puebla, E.; Monge, M. A. *Angew. Chem., Int. Ed.* **2006**, *45*, 7998−8001.
(18) Zhao, X. Bu, X. Wu, T. Zheng, S.-T. Weng, L. Feng, P. *Nat. Commun.* **2013**, *4*, article 2344, 10.1038/ncomms3344.
(19) Wang, S.; Alekseev, E. V.; Diwu, J.; Casey, W. H.; Phillips, B. L.; Depmeier, W.; Albrecht-Schmitt, T. E. *Angew. Chem., Int. Ed.* **2010**, *49*, 1057−1060.
(20) Custelcean, R. *Chem. Soc. Rev.* **2010**, *39*, 3675−3685 and references therein.
(21) Tran, D. T.; Zavalij, P. Y.; Oliver, S. R. J. *J. Am. Chem. Soc.* **2002**, *124*, 3966−3969.
(22) Swanson, C. H.; Shaikh, H. A.; Rogow, D. L.; Oliver, A. G.; Campana, C. F.; Oliver, S. R. J. *J. Am. Chem. Soc.* **2008**, *130*, 11737−11741.
(23) Fei, H.; Oliver, S. R. J. *Angew. Chem., Int. Ed.* **2011**, *50*, 9066−9070.
(24) (a) Fei, H.; Pham, C. H.; Oliver, S. R. J. *J. Am. Chem. Soc.* **2012**, *134*, 10729−10732. (b) Fei, H.; Han, C. S.; Robins, J. C.; Oliver, S. R. J. *Chem. Mater.* **2013**, *25*, 647−652.
(25) Swanson, C. H.; Abdollahian, Y.; Shaikh, H. A.; Ikehata, M.; Rogow, D. L.; Oliver, S. R. J. *Cryst. Growth Des.* **2012**, *12*, 93−98.
(26) Shimizu, G. K. H.; Vaidhyanathan, R.; Talyor, J. M. *Chem. Soc. Rev.* **2009**, *38*, 1430−1449.
(27) Millange, F.; Walton, R. I.; Lei, L.; O'Hare, D. *Chem. Mater.* **2000**, *12*, 1990−1994.
(28) Crepaldi, E. L.; Tronto, J.; Cardoso, L. P.; Valim, J. B. *Colloids Surf., A* **2002**, *211*, 103−114.
(29) Gu, J.-Z.; Lu, W.-G.; Jiang, L.; Zhou, H.-C.; Lu, T.-B. *Inorg. Chem.* **2007**, *46*, 5835−5837.

DOI: 10.1021/acs.inorgchem.5b00073
Inorg. Chem. 2015, 54, 3883−3888